Specific Surface Area Increase during Cellulose Nanofiber Manufacturing Related to Energy Input

Carl Moser,[a,b] Gunnar Henriksson,[a] and Mikael E. Lindström [a,*]

Softwood fibers pretreated with a monocomponent endoglucanase were used to prepare a series of cellulose nanofiber qualities using a microfluidizer and 2 to 34 MWh ton^{-1} of energy input. The specific surface area was determined for the series using critical point drying and gas adsorption. Although the specific surface area reached a maximum of 430 m^2 g^{-1} at 11 MWh ton^{-1}, the nanofiber yield and transmittance continued to increase beyond this point, indicating that more energy is required to overcome possible friction caused by an interwoven nanofiber network unrelated to the specific surface area. A new method for estimating the surface area was investigated using xyloglucan adsorption in pure water. With this method it was possible to follow the disintegration past the point of maximum specific surface area. The technical significance of these findings is discussed.

Keywords: Cellulose nanofibers; Cellulose; Nano; Xyloglucan; Specific surface area; Homogenization

*Contact information: a: Department of Fibre and Polymer Technology, School of Chemistry, Royal Institute of Technology, KTH, Teknikringen 56-58, 10044, Stockholm, Sweden; b: Valmet AB, 851 94 Sundsvall, Sweden; *Corresponding author: mil@kth.se*

INTRODUCTION

Cellulose nanofibers are presently the subject of intensive study, both in academia and industry. Cellulose, the main structural component of wood fibers, is organized in several hierarchical levels (Mühlenthaler 1949; Meier 1962), ranging from an assembly of partly crystalline elementary fibrils containing 18 to 36 cellulose chains (Doblin *et al.* 2002; Fernandes *et al.* 2011; Hill *et al.* 2014) with a lateral dimension ranging from 3 to 5 nm (Meier 1962; Ohad and Danon 1964; Blackwell and Kolpak 1975), to aggregates of elementary fibrils with diameters of 15 to 40 nm (Saxena and Brown 2005; Eichhorn *et al.* 2010). Turbak *et al*. (1983) and Herrick *et al.* (1983) developed a method for disintegrating chemical pulp into cellulose nanofibers by utilizing a high-pressure homogenizer; however, due to the high energy consumption of the process and a lack of interest in this nanomaterial, at the time, cellulose nanofiber development did not gain momentum for almost three decades. Facilitation of the disintegration using pretreatments such as monocomponent endoglucanase enzymes (Henriksson *et al.* 2007) or TEMPO-mediated oxidation (Saito *et al.* 2007) increased the processability resulting in a lower energy consumption. Unfortunately, the study of cellulose nanofibers became characterized by terminological ambiguity due to the renewed interest and development of pretreatments, as the quantity of various fibrous entities is highly dependent on both the pretreatment and production methods (Klemm *et al.* 2011). In this work, an inhomogeneous mixture of differently sized nanofibers was studied, and the term "cellulose nanofibers (CNF)" was chosen because it represents a wide range of fibrous nanoparticles that comprise cellulose.

Many important questions remain with respect to the CNF manufacturing process. However, cellulose is the predominant chemical compound in pulp fiber, and it seems plausible that CNF is generated by cellulose surfaces separating from each other. In enzymatic or untreated pulps, this process is based on breaking non-covalent bonds (hydrogen bonds and phi interactions) (Lindman *et al.* 2010). These bonds and the energy required to break them are negligible when considering chemical pretreatments that can increase the charge density beyond 1.5 meq g^{-1} (Tejado *et al.* 2012).

The well-established method for measuring specific surface area (SSA) using gas adsorption and the theories stipulated by Brunauer, Emmett and Teller 1938 (BET) requires a dry substrate. Drying cellulose-based material leads to internal collapse and aggregation that significantly reduces the SSA (Scallan 1974) even when employing methods such as lyophilization. A solvent exchange procedure and critical point drying can to a large extent keep the original structure (Svensson *et al.* 2013); however, a method that can measure the SSA of the cellulose in a wet state is preferable. One viable route is adsorption of Congo red molecules to cellulose (Inglesby and Zeronian 1996; Ougiya *et al.* 1998; Nge *et al.* 2013), except that the required ionic strength can induce CNF aggregation/gelation (Fall *et al.* 2011). Xyloglucan (XG) is a water-soluble polysaccharide that specifically adsorbs to cellulose (Hayashi *et al.* 1994) independent of pH and ionic strength (Mishima *et al.* 1998). Zhou *et al.* 2006, showed a relationship between free cellulose surface area and xyloglucan adsorption, indicating a potential alternative for evaluating surfaces of cellulosic nanomaterials. Adsorption of xyloglucan is commonly measured using Quartz Crystal Microbalance (QCM) or Surface Plasmon Resonance (SPR) (Eronen *et al.* 2011); however, the concentration can also be measured in solution by color formation when complexing with iodine (Christiernin *et al.* 2003) or dried by sugar analysis (Prakobna *et al.* 2015c). Other possible approaches include adsorption of galactoglucomannan (Prakobna *et al.* 2015b) and starch (Prakobna *et al.* 2015a), although the mechanisms for starch adsorption are highly dependent on the charge density of the cellulose and the starch molecule (Kontturi *et al.* 2008).

In this work, the relationship between the amount of energy consumed in the cellulose nanofiber manufacturing process (homogenization) and the increase in the specific surface area (SSA) was estimated using a theoretical value for the strength of a cellulose-cellulose bond (Bergenstråhle *et al.* 2008). Transmittance and nanofiber yield was shown to be related to the degree of disintegration and is here utilized to follow the disintegration process (Moser *et al.* 2015).

EXPERIMENTAL

Materials

CNF was produced from a once-dried mixed softwood kraft pulp (SCA Östrand, Sundsvall, Sweden) with 16.7% hemicellulose and 0.65% lignin and a DP of 2600. Xyloglucan was purified from tamarind kernel powder by sequential centrifugation and dilution with deionized water and the purified product contained 89% of 780k M_w (Polydispersity index (PDI) 1.86), 6% of 180k M_w (PDI 1.01), and 5% of 6k M_w (PDI 1.01). All other chemicals were of analytical grade.

Homogenization

The reactivity of the dried pulp was increased by PFI refining (10% dry content) at 230 kWh ton^{-1}. Enzymatic hydrolysis was performed at 25 ECU g^{-1} using 490 kWh ton^{-1} (heating) to deactivate the enzymes, according to the procedure described by Moser *et al.* 2015. Fibrillation was achieved in a microfluidizer (M-110EH, Microfluidics Corp., Westwood, USA) at a pulp concentration of 15 g L^{-1} with a pressure of 900 Bar for the first pass in 400/200 µm chambers, corresponding to 1.5 MWh ton^{-1} and 1600 Bar for the second and subsequent passes in 200/100 µm chambers, corresponding to 3.2 MWh ton-1 per pass. A sample was collected after each pass, and the pulp was subjected to a total of 11 passes (2-34 MWh ton^{-1}).

Calculation of Energy Consumption

The homogenization energy was estimated using Bernoulli's equation with the assumptions of unchanged dynamic energy and absence of heat generation, according to (Ankerfors 2015).

Measurement of Cellulose Surface Area by Krypton Gas Adsorption

Each CNF sample was diluted to 0.1 g L^{-1} using an Ultra-Turrax device (®T25 digital, IKA, Staufen, Germany) at 10k RPM for 10 min. For each sample, 200 mL was deaerated and filtered on a 0.45 µm PVDF membrane (Durapore®), and the 45 g m^{-2} films were removed once a freestanding film was formed (approximately 4% dry content). Water was solvent-exchanged for 96% ethanol for 24 h, and then 99.9% ethanol in three steps of 24 h each before being subjected to critical point drying (liquid CO_2) in an Autosamdri-815 device (Tousimis Research Co., Rockville, USA), using 10 min of purge time. The specific surface area (m^2 g^{-1}) was determined using Krypton (Kr, 202 pm van der Waals radii) adsorption in a Micromeritics ASAP 2020 analyzer (Norcross, USA) according to the BET theory; two measurements were recorded for each sample (Brunauer *et al.* 1938).

Calculation of Energetic Efficiency of the Homogenization Process

The theoretical energy required to increase the surface area was calculated using 8.33×10^{-8} kWh m^{-2} as the energy required to break a cellulose-cellulose bond and replace it with a cellulose-water bond (Bergenstråhle *et al.* 2008). The efficiency of the homogenization was calculated by dividing the theoretical value by the measured value for the obtained increase in specific surface area.

Xyloglucan Adsorption

Native xyloglucan was added to 400 µL CNF (0.1 g L^{-1}) and diluted to a final volume of 2 mL. The samples were incubated for 96 h after 200 µL of the sample was taken out and 1 mL color reagent was added (containing 1 mL 20% $NaSO_4$, 200 µL 1% KI, and 0.5% I_2) (Christiernin *et al.* 2003). The samples were centrifuged for 4 min at 14.1 RCF (relative centrifugal force) and kept in the dark for 30 min before measurement of absorbance at 660 nm on a UV-Vis spectrophotometer (UV-2550, Shimadzu, Kyoto, Japan). The amount adsorbed xyloglucan was calculated by comparison with a xyloglucan sample without CNF.

Yield and Transmittance

The nanofiber yield was measured as the fraction of the CNF in the supernatant after centrifugation of a 0.1 g L^{-1} CNF at 9800 RCF using an Eppendorf Minispin Plus (Hamburg, Germany). Transmittance was measured for 0.1 g L^{-1} CNF solutions in 1 cm glass cuvettes at a set wavelength of 500 nm in a UV-Vis spectrophotometer (UV-2550, Shimadzu).

RESULTS AND DISCUSSION

The specific surface area of the chemical pulp was measured using the BET method, subjecting it to a series of homogenizations at approximately 11 MWh ton^{-1}. The maximum value was 430 m^2 g^{-1}, with no increase observed beyond this value, as shown in Fig. 1 A. A specific surface area of 430 m^2 g^{-1} corresponds to an average lateral size of 5 nm (Svensson *et al.* 2013), indicating that the fibers were almost fully fibrillated after the 11 MWH ton^{-1} treatment; however, both the nanofiber yield measured by centrifugation and transmittance continued to increase with additional energy input beyond this point (Fig. 2), showing that fibrillation continued. The observation that the maximum surface area was obtained at such an early point indicates that the internal structure of the remaining fibers reached a maximum "swollen state," where the fibrils are sufficiently separated to allow krypton molecules to adsorb, but they remain in larger structures that are at least partly still attached (possibly by friction) to an interwoven network of nanofibers or certain nodes with molecular contact.

The reference sample that was treated with only high-consistency refining exhibited a surface area of 199 m^2 g^{-1}, higher than the previously reported 128 m^2 g^{-1} value for un-dried pulp (Svensson *et al.* 2013), indicating that high-consistency refining of the once-dried fibers was more than sufficient for recovering the surface area that was lost during drying. The value for the reference sample corresponds to lateral dimensions of 11.7 nm, smaller than the approximately 36 nm obtained for native aggregates (Svensson *et al.* 2013). This result showed that the original structure was significantly swollen by mechanical treatment.

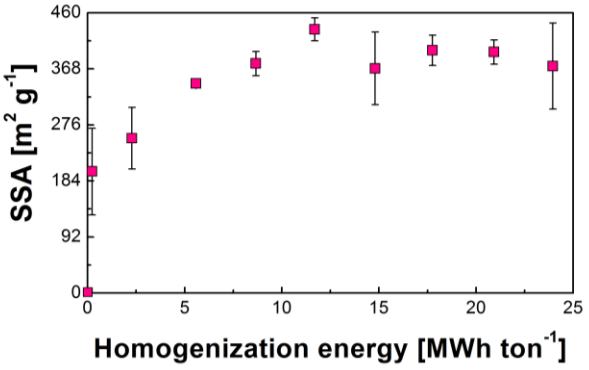

Fig. 1. Specific surface area *versus* energy of the fiber treatment; error bars correspond to the standard deviation for the two measured samples

The efficiency for increasing the SSA was highest on the first pass (2300 kWh $tonne^{-1}$) at 0.29% and decreased upon further passes. Because the efficiency is related to

finite increases in the surface area, this value is not directly related to the actual amount of nanofibers, but rather to the degree of swelling. Rapid acceleration in the interface of the chambers could impose enough force on the fibers to cause fibrillation until the velocity of the fiber became equilibrated, leaving fiber fragments that were not disintegrated. This phenomenon can partly explain the low efficiency. The low efficiency also indicates that this process caused breakage of the covalent bonds in the fibers, consuming energy. Another source of low efficiency may be an underestimation of the heat generated from the pump and in the chambers; this in turn causes an error in the calculations for the energy consumption, so that lower values would be obtained if the generated heat was taken into account.

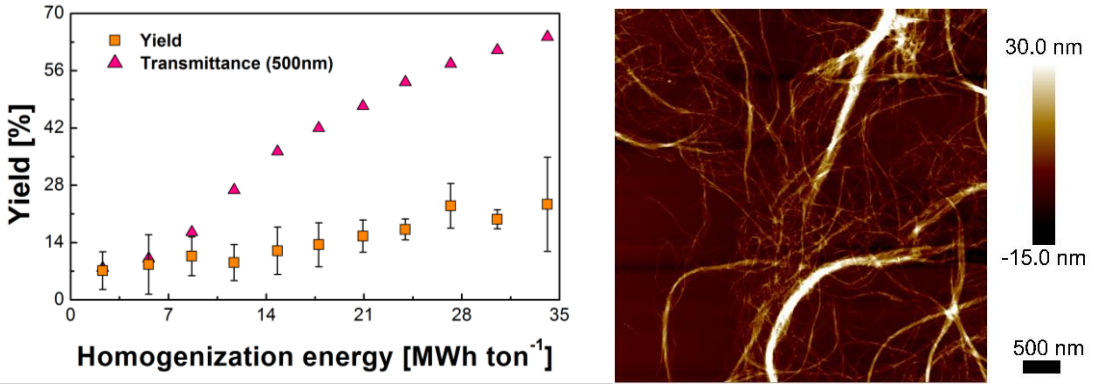

Fig. 2. Left: Both transmittance and yield exhibited a continuous increase with increasing homogenization energy. **Right:** AFM image of the smallest nanofibers regarded as 'yield', with an average width of 6.1±1.1 nm. Image was taken using a Multimode 8 (Bruker, USA) instrument utilizing ScanAsyst. Error bars correspond to Student's t confidence intervals.

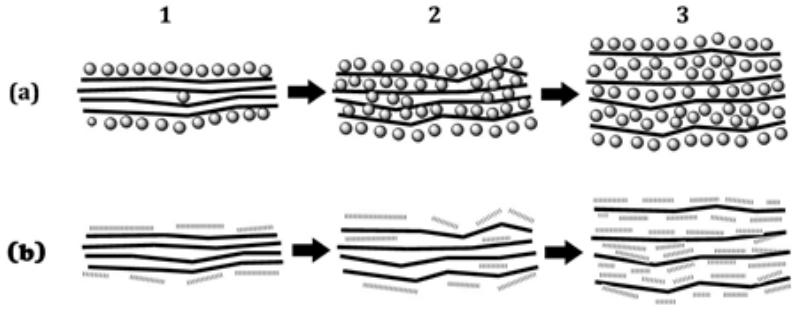

Fig. 3. Hypothesis for the binding of Kr (a) and XG (b) during homogenization: before homogenization (1) fibrillary aggregates are closely bound together, limiting the area capable of maintaining either molecule. Upon homogenization, these fibrillary aggregates are gradually separated and in the intermediate phase, (2) pores and cavities are created that are sufficiently large for Kr atoms to penetrate, while the larger XG molecules can only access a part of the newly exposed areas. After more intensive homogenization (3), the cellulose aggregates separate further, allowing XG to bind to accessible surfaces, whereas the amount of adsorbed Kr-atoms remains fairly constant.

The lack of an increase in the SSA measured using Kr adsorption before full fibrillation was achieved suggests that although surfaces are created, they stay closely associated with each other. With further homogenization, the same surfaces fully separate, leading to an increase in yield and transmittance (Fig. 3). By using a molecule larger than Kr, it is possible to observe a shift in the peak for the maximum SSA, as can be seen from

the xyloglucan adsorption measurements (Fig. 4). The amount of adsorbed xyloglucan was proportional to the energy input beyond the energy corresponding to the maximum SSA value. The surface accessible to the krypton is generally larger than the surface available for the xyloglucan molecules due to the size difference and this gives a reasonable explanation for the continuous adsorption of xyloglucan while the krypton reaches a maximum.

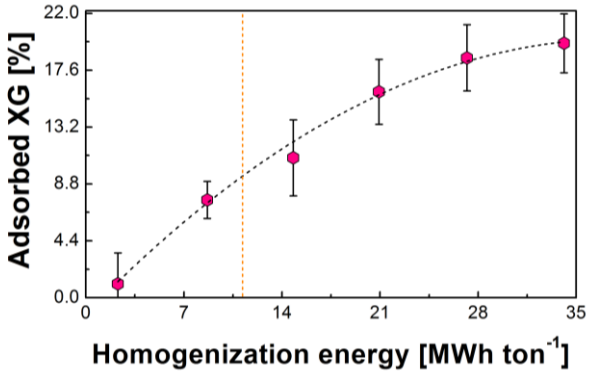

Fig. 4. Xyloglucan adsorption for samples incubated 96 h; error bars correspond to Student's t confidence intervals. Second degree polynomial fit R^2=0.992. The horizontal line represents the point were no further increase in SSA was observed for the BET measurement.

Measurement of the cellulose surface with XG adsorption has some advantages relative to the BET approach; namely, experiments are simple and can be performed on wet cellulose samples. However, the XG used in this study was heterogeneous with respect to molecular weight, and SSA calibrations were therefore difficult.

CONCLUSIONS

1. The low efficiency for increasing the specific surface area using homogenization indicates that disintegrating cellulosic fibers into nanofibers is not governed just by separation of the nanofibers from each other. Instead, it could be partly explained by the fact that energy is required to disrupt the interwoven network of nanofibers.
2. In contrast to BET measurements, xyloglucan adsorption increases with energy input without plateauing. This is a novel method for measuring the surface area of wet CNF.

ACKNOWLEDGMENTS

This work was supported by Valmet Corporation and FORIC. The authors thank professor Lars Wågberg, Royal Institute of Technology, for his kind advice and interest in this work.

REFERENCES CITED

Ankerfors, M. (2015). *Microfibrillated Cellulose. Energy-Efficient Preparation Techniques and Applications in Paper*, Dissertation, KTH Royal Institute of Technology.

Bergenstråhle, M., Mazeau, K., and Berglund, L. A. (2008). "Molecular modeling of interfaces between cellulose crystals and surrounding molecules: Effects of caprolactone surface grafting," *Eur. Polym. J.*, 44(11), 3662-3669. DOI: 10.1016/j.eurpolymj.2008.08.029

Blackwell, J., and Kolpak, F. J. (1975). "The cellulose microfibril as an imperfect array of elementary fibrils," *Macromolecules* 8(3), 322-326. DOI: 10.1021/ma60045a015

Brunauer, S., Emmet, P. H., and Teller, E. (1938). "Adsorption of gases in multimolecular layers," *J. Am. Chem. Soc.* 60(2), 309-319. DOI: 10.1021/ja01269a023

Christiernin, M., Henriksson, G., Lindström, M. E., Brumer, H., Teeri, T. T., Lindstrom, T., and Laine, J. (2003). "The effects of xylogucan on the properties of paper made from bleached kraft pulp," *Nord. Pulp Paper Res.*, 18(2), 182-187.

Doblin, M. S., Kurek, I., Jacob-Wilk, D., and Delmer, D. P. (2002). "Cellulose biosynthesis in plants: From genes to rosettes," *Plant Cell Physiol.* 43(12), 1407-1420. DOI: 10.1093/pcp/pcf164

Eichhorn, S. J., Dufresne, A., Aranguren, M., Marcovich, N. E., Capadona, J. R., Rowan, S. J., Weder, C., Thielemans, W., Roman, M., Renneckar, S., Gindl, W., Veigel, S., Keckes, J., Yano, H., Abe, K., Nogi, M., Nakagaito, A. N., Mangalam, A., Simonsen, J., Benight, A. S., Bismarck, A., Berglund, L. A., and Peijs, T. (2010). "Review: Current international research into cellulose nanofibres and nanocomposites," *J. Mater. Sci.* 45(1), 1-33. DOI: 10.1007/s10853-009-3874-0

Eronen, P., Junka, K., Laine, J., and Österberg, M. (2011). "Interaction between water soluble polysaccharides and native nanofibrillar cellulose thin films," *Bioresources* 6(4), 4200-4217.

Fall, A. B., Lindström, S. B., Sundman, O., Ödberg, L., and Wågberg, L. (2011). "Colloidal stability of aqueous nanofibrillated cellulose dispersions," *Langmuir* 27(18), 11332-11338. DOI: 10.1021/la201947x

Fernandes, A. N., Thomas, L. H., Altaner, C. M., Callow, P., Forsyth, V. T., Apperley, D. C., Kennedy, C. J., and Jarvis, M. C. (2011). "Nanostructure of cellulose microfibrils in spruce wood," *Proceedings of the National Academy of Sciences of the United States of America* 108(47), 195-203. DOI: 10.1073/pnas.1108942108

Hayashi, T., Ogawa, K., and Mitsuishi, Y. (1994). "Characterization of the adsorption of xylogucan to cellulose," *Plant Cell Physiol.* 35(8), 1199-1905.

Henriksson, M., Henriksson, G., Berglund, L. A., and Lindström, T. (2007). "An environmentally friendly method for enzyme-assisted preparation of microfibrillated cellulose (MFC) nanofibers," *Eur. Polym. J.* 43(8), 3434-3441. DOI: 10.1016/j.eurpolymj.2007.05.038

Hill, J. L., Hammudi, M. B., and Tien, M. (2014). "The *Arabidopsis* cellulose synthase complex: A proposed hexamer of CESA trimers in an equimolar stoichiometry," *Plant Cell* 26(12), 4834-4842. DOI: 10.1105/tpc.114.131193

Inglesby, M. K., and Zeronian, S. H. (1996). "The accessibility of cellulose as determined by dye adsorption," *Cellulose* 3(1), 165-181. DOI: 10.1007/BF02228799

Klemm, D., Kramer, F., Moritz, S., Lindström, T., Ankerfors, M., Gray, D., and Dorris, A. (2011). "Nanocelluloses: A new family of nature-based materials," *Angew. Chem. Int. Ed.* 50(24), 5438-5466. DOI: 10.1002/anie.201001273

Kontturi, K. S., Tammelin, T., Johansson, L.-S., and Stenius, P. (2008). "Adsorption of cationic starch on cellulose studied by QCM-D," *Langmuir* 24(9), 4743-4749. DOI: 10.1021/la703604j

Lindman, B., Karlström, G., and Stigsson, L. (2010). "On the mechanism of dissolution of cellulose," *J. Mol. Liq.* 156(1), 76-81. DOI: 10.1016/j.molliq.2010.04.016

Meier, H. (1962). "Chemical and morphological aspects of the fine structure of wood," *Pure Appl. Chem.* 5, 37-52.

Mishima, T., Hisamatsu, M., York, W. S., Teranishi, K., and Yamada, T. (1998). "Adhesion of beta-d-glucans to cellulose," *Carbohyd. Res.* 308(3-4), 389-395.

Moser, C., Lindström, M., and Henriksson, G. (2015). "Toward industrially feasible methods for following the process of manufacturing cellulose nanofibers," *BioResources* 10(2), 2360-2375. DOI: 10.15376/biores.10.2.2360-2375

Mühlenthaler, K. (1949). "Electron micrographs of plant fibers," *Biochim. Biophys. Acta*, 3(15), 15-25. DOI: 10.1016/0006-3002(49)90075-X

Nge, T. T., Lee, S.-W., and Endo, T. (2013). "Preparation of nanoscale cellulose materials with different morphologies by mechanical treatments and their characterization," *Cellulose* 20(4), 1841-1852. DOI: 10.1007/s10570-013-9962-y

Ohad, I., and Danon, D. (1964). "On the dimensions of cellulose microfibrils," *J. Cell Biol.* 22(1), 302-305. DOI: 10.1083/jcb.22.1.302

Ougiya, H., Hioki, N., Watanabe, K., Morinaga, Y., Yoshinaga, F., and Samejima, M. (1998). "Relationship between the physical properties and surface area of cellulose derived from adsorbates of various molecular sizes," *Biosci. Biotechnol. Biochem.* 62(10), 1880-1884. DOI: 10.1271/bbb.62.1880

Prakobna, K., Galland, S., and Berglund, L. A. (2015a). "High-performance and moisture-stable cellulose-starch nanocomposites based on bioinspired core-shell nanofibers," *Biomacromolecules* 16(3), 904-912. 10.1021/bm5018194

Prakobna, K., Kisonen, V., Xu, C., and Berglund, L. A. (2015b). "Strong reinforcing effects from galactoglucomannan hemicellulose on mechanical behavior of wet cellulose nanofiber gels," *Journal of Materials Science* 50(22), 7413-7423. 10.1007/s10853-015-9299-z

Prakobna, K., Terenzi, C., Zhou, Q., Furo, I., and Berglund, L. A. (2015c). "Core-shell cellulose nanofibers for biocomposites - Nanostructural effects in hydrated state," *Carbohyd. Polym.* 125, 92-102. 10.1016/j.carbpol.2015.02.059

Saito, T., Kimura, S., Nishiyama, Y., and Isogai, A. (2007). "Cellulose nanofibers prepared by TEMPO-mediated oxidation of native cellulose," *Biomacromolecules* 8(8), 2485-91. DOI: 10.1021/bm0703970

Saxena, I. M., and Brown, R. M. (2005). "Cellulose biosynthesis: Current views and envolving concepts," *Anals. Bot.* 96(1), 9-21. DOI: 10.1093/aob/mci155

Scallan, A. M. (1974). "The structure of the cell wall of wood: A consequence of anisotropic inter-microfibrillar bonding?" *Wood Sci.* 6(3), 266-271.

Svensson, A., Larsson, P. T., Salazar-Alvarez, G., and Wagberg, L. (2013). "Preparation of dry ultra-porous cellulosic fibres: Characterization and possible initial uses," *Carbohyd. Polym.* 92(1), 775-783. DOI: 10.1016/j.carbpol.2012.09.090

Tejado, A., Alam, M. N., Antal, M., Yang, H., and van de Ven, T. G. M. (2012). "Energy requirements for the disintegration of cellulose fibers into cellulose nanofibers," *Cellulose* 19(3), 831-842. DOI: 10.1007/s10570-012-9694-4

Zhou, Q., Baumann, M., Brumer, H., and Teeri, T. (2006). "The influence of surface chemical composition on the adsorption of xyloglucan to chemical and mechanical pulps," *Carbohyd. Polym.* 63(4), 449-458. 10.1016/j.carbpol.2005.09.015

Article submitted: March 7, 2016; Peer review completed: May 9, 2016; Revised version received: June 27, 2016; Accepted: June 28, 2016; Published: July 12, 2016.
DOI: 10.15376/biores.11.3.7124-7132